Radioactive Decay Speedup at $T = 5$ K: Electron-Capture Decay Rate of ^{7}Be Encapsulated in C_{60}

T. Ohtsuki,[1] K. Ohno,[2] T. Morisato,[3] T. Mitsugashira,[4] K. Hirose,[1] H. Yuki,[1] and J. Kasagi[1]

[1]*Laboratory of Nuclear Science, Tohoku University, Mikamine, Taihaku-ku, Sendai 982-0826, Japan*

[2]*Department of Physics, Yokohama National University, Tokiwadai, Hodogaya-ku, Yokohama 240-8501, Japan*

[3]*Accelrys K.K., 3-3-1 Nishishinbashi, Minato-ku, Tokyo 105-0003, Japan*

[4]*IMR, Tohoku University, Narita, Oarai, Ibaraki 311-1313, Japan*

(Received 14 September 2006; revised manuscript received 2 December 2006; published 18 June 2007)

The electron-capture (EC) decay rate of ^{7}Be in C_{60} at the temperature of liquid helium ($T = 5$ K) was measured and compared with the rate in Be metal at $T = 293$ K. We found that the half-life of ^{7}Be in endohedral C_{60} (^{7}Be@C_{60}) at a temperature close to $T = 5$ K is 52.47 ± 0.04 d, a value that is 0.34% faster than that at $T = 293$ K. In this environment, the half-life of ^{7}Be is nearly 1.5% faster than that inside Be metal at room temperature ($T = 293$ K). We then interpreted our observations in terms of calculations of the electron density at the ^{7}Be nucleus position inside the C_{60}; further, we estimate theoretically the temperature dependence (at $T = 0$ K and 293 K) of the electron density at the Be nucleus position in the stable center inside C_{60}. The theoretical estimates were almost in agreement with the experimental observations.

DOI: 10.1103/PhysRevLett.98.252501 PACS numbers: 21.10.Tg, 23.40.Hc, 27.20.+n, 36.40.Cg

In nuclear β-decay and in the closely related process of electron capture (EC), the decay curve is an exponential function versus time with a constant decay rate. The decay rate from any parent state, usually the nuclear ground state, to any final daughter state is proportional to the product of a nuclear matrix element and factors related to the phase-space available to the neutrino and electron and to the overlap between the initial electron and final nuclear wave functions. Segré *et al.* [1,2] were the first to suggest that since the latter factors depend on the environment in which the transmutation occurs, the decay rate should depend on factors such as chemical form, pressure, and temperature. It has been a long-standing challenge to establish the degree to which manipulation of these environmental factors can, in practice, change nuclear decay rates [3–16].

Recently we measured the half-life of ^{7}Be in endohedral C_{60} (^{7}Be@C_{60}) and reported that the decay rate increases by almost 0.8% compared to that in Be metal [Be metal (^{7}Be)] [17,18]. This fact implied that the ^{7}Be atoms are located in a unique environment inside C_{60}. Several factors contribute to this environment: the many π electrons of C_{60}, special dynamic motions inside C_{60}, etc. Therefore, it is intriguing to study the temperature dependence of the half-life of ^{7}Be inside C_{60}. In the present study, in order to suppress the dynamic motion of ^{7}Be inside C_{60}, we measured the half-life of ^{7}Be in ^{7}Be@C_{60} that had been cooled to a temperature close to liquid helium ($T = 5$ K). We also present calculations of the electron density at the ^{7}Be nucleus position at the site inside C_{60} at different temperatures (at $T = 0$ K and 293 K). The theoretical estimates reveal the stable position of the ^{7}Be nucleus inside C_{60} and the temperature dependence of the electron density at the ^{7}Be nuclear position.

One way to produce atom endohedral C_{60} is to insert foreign atoms into preexisting C_{60} [19–21]. We produced an endohedral C_{60} by nuclear recoil implantation [17,18]. Recently, we developed a reference method to measure the half-life of ^{7}Be inside C_{60} and that in Be metal, as shown in Fig. 1(a). The method used to produce the ^{7}Be@C_{60} and ^{7}Be reference samples has been described previously [18]. In order to measure the half-life at $T = 5$ K, the ^{7}Be@C_{60} sample was placed in the top of a He closed-cycle cryostat. The two samples, ^{7}Be@C_{60} (fastened in the cryostat) and Be metal (^{7}Be), were placed in a computer-controlled sample changer, which moved the samples precisely in front of a γ-ray detector as shown in the figure. The measurement was started after the ^{7}Be@C_{60} sample underwent sufficient cooling at $T = 5$ K in the vacuum state. This arrangement allowed the decay rates of the two samples to be measured in a consistent fashion while reducing systematic errors. In the system, the internal clock time of the computer for data acquisition was constantly calibrated by a time-standard signal distributed via a long-wave radio center in Japan. The 478 keV γ rays emanating from the EC-decay daughter of ^{7}Be were measured using a high-purity germanium (HPGe) detector (ΔE_{FWHM} is 1.8 keV and has 50% relative efficiency) coupled to a 2048- and/or 4096-channel pulse-height analyzer. Here, we set the specific measurement duration to 21 600 s (21 480 s for the live measurement time and 120 s for the dead time of the measurement system plus the sample exchange) for one data point. In Fig. 1(b), a typical γ-ray spectrum obtained in the measurement of the ^{7}Be decay inside C_{60} is shown as a function of γ-ray energy in keV. The amount of radioactivity associated with the decay of ^{7}Be ($E_\gamma = 478$ keV) could be uniquely analyzed through the identification of characteristic γ rays.

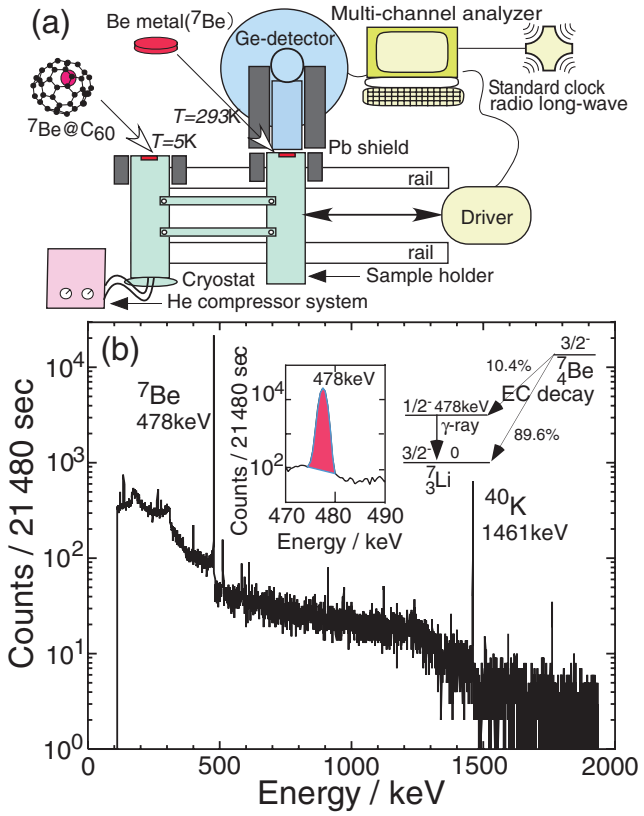

FIG. 1 (color). (a) Experimental setup for the measurement of the half-lives of ^{7}Be in the ^{7}Be@C$_{60}$ and of the ^{7}Be reference metal. (b) Typical γ-ray spectrum of ^{7}Be in the sample of ^{7}Be@C$_{60}$ cooled down to $T = 5$ K.

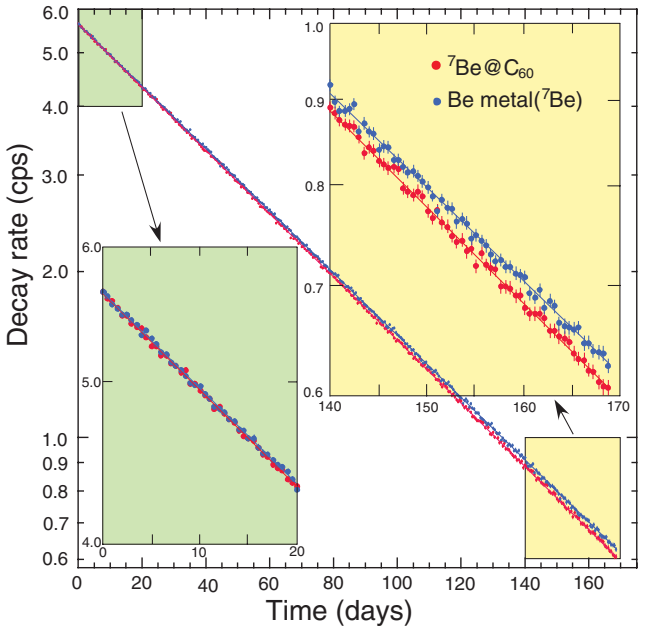

FIG. 2 (color). Exponential decay curves of ^{7}Be in samples of the ^{7}Be@C$_{60}$ at $T = 5$ K (red circles) and the Be metal (^{7}Be) at $T = 293$ K (blue circles). Insets corresponding to the decay intervals of 0–20 d and 140–170 d are displayed with an expanded scale.

Figure 2 shows two exponential decay curves of the ^{7}Be radioactivities for samples of ^{7}Be@C$_{60}$ and Be metal (^{7}Be) plotted versus time (in days). In order to compare the decay curves in Fig. 2, the data for the ^{7}Be@C$_{60}$ were normalized to those for the Be metal (^{7}Be) at Time = 0, which was 5.17 counts/s (cps) for the ^{7}Be@C$_{60}$ and 5.65 cps for the Be metal (^{7}Be). Red and blue circles indicate the radioactivities (decay rate in cps) for the samples of ^{7}Be@C$_{60}$ at $T = 5$ K and Be metal (^{7}Be) at $T = 293$ K, respectively. The decay curves obtained in the present measurements were fitted, by use of the MINUIT program distributed by the CERN Program Library. The statistical error dominates the uncertainty for each data point shown in Fig. 2. The uncertainty of our measurement corresponds to the uncertainty of the slope of the straight line fitted to the logarithm of the counts (i.e., counts per second) of the decay spectrum. The reduced chi-square values of the exponential fits are between 0.90 and 1.12. The uncertainty due to the dead time was estimated to be less than 0.04%, and the systematic error in the measurements was estimated to be less than half of the statistical error quoted above [18]. We have measured the decay rates and deduced the corresponding half-lives of ^{7}Be in samples of ^{7}Be@C$_{60}$ (at $T = 5$ K) and in Be metal (^{7}Be) (at $T = 293$ K) in two separate measurements with durations of 168 d and 143 d. In Fig. 3, the red circles indicate the half-lives obtained for the sample of ^{7}Be@C$_{60}$ at $T = 5$ K and the blue circles indicate those of the Be metal (^{7}Be) at $T = 293$ K. Green circles indicate the half-lives in ^{7}Be@C$_{60}$ from the previous study [18]. The half-life of ^{7}Be in ^{7}Be@C$_{60}$ (at $T = 5$ K) averaged over two runs was 52.47 ± 0.04 d.

On the other hand, the half-life of ^{7}Be in the Be metal (^{7}Be) averaged over many measurements was

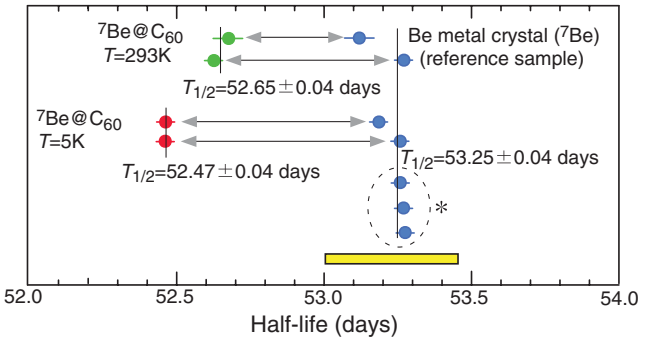

FIG. 3 (color). Half-lives ($T_{1/2}$) measured in this time period are plotted as red circles for the ^{7}Be@C$_{60}$ at $T = 5$ K. The green circles are half-lives measured previously at $T = 293$ K ($T = 293$ K) (previous work [18]). The blue circles represent the half-lives used as reference samples of Be metal (^{7}Be) (e.g., shown by arrows). Points shown by the asterisk are the half-lives of Be metal (^{7}Be) samples compared to other samples [22]. Half-lives previously measured span the thick yellow bar.

53.25 ± 0.04 d [22]. The half-lives obtained for ^{7}Be in several other host materials and chemical forms such as graphite, gold, oxide, etc., have been presented by many works [3–16]. In Fig. 3, half-lives previously measured are also shown by a thick yellow bar as a comparison. The half-lives mostly range between 53.10 and 53.40 d [6,10,12–15]. Therefore, we find that our reference measurement of the half-life for ^{7}Be in Be metal (^{7}Be) is in satisfactory agreement with other available data.

It is surprising to note that the difference between the half-life of ^{7}Be in the ^{7}Be@C_{60} at $T = 5$ K and that in the Be metal (^{7}Be) at $T = 293$ K was more dramatic than that between the half-life of ^{7}Be in the ^{7}Be@C_{60} at $T = 293$ K and that in the Be metal (^{7}Be) at $T = 293$ K as shown in Fig. 3. Here, the former half-life at $T = 5$ K was almost 1.5% shorter than that for the Be metal (^{7}Be) sample at $T = 293$ K. It can be clearly seen in the figure that the half-life of ^{7}Be in the ^{7}Be@C_{60} (at $T = 5$ K) is 0.34% shorter than that in the ^{7}Be@C_{60} under $T = 293$ K and shorter than any ^{7}Be half-life reported in any environment up to now.

Since the EC-decay rate depends on the electron density at the nucleus position, we calculated the electron density at the ^{7}Be nucleus position inside the C_{60}. In order to correctly express the cusplike profile of the electron density near the nucleus position, we adopted the first-principles calculation program, DMOL3 [23], using numerical, localized orbitals as a basis set. Our calculation is based on the generalized gradient approximation (GGA) called BLYP [24,25] for the exchange-correlation potential of the density functional theory. We used a double-numeric quality basis set with polarization functions (DNP). We first calculated the total energy of the Be atom for various positions inside the C_{60}. From this calculation, we identified four positions of the Be atom having relatively low total energies; from the lowest to the fourth lowest in total energy, the Be atom is located at the C_{60} center, under a five-membered ring, under a single bond, and under a six-membered ring. Then, starting from these four Be geometries, we performed a structural optimization of the whole system and redetermined the total energy and the electron density at the Be nucleus position after relaxation at $T = 0$ K. We also determined the electron density (at the ^{7}Be nucleus position) for an isolated Be atom and for Be metal. All the results are listed in Table I. From Table I, it is clear that the most stable position of the Be atom inside the C_{60} is the center, and the electron density at the Be nucleus position is the highest in this case. The electron density at the Be nucleus position changes from higher to lower depending on the Be position as follows: C_{60} center $>$ Be atom $>$ Be metal $>$ other sites inside C_{60}.

At the C_{60} center, the Be atom is almost isolated with no bonds with the surrounding carbon atoms as seen in Fig. 4 (upper left). The electronic wave function of the Be2s highest-occupied-molecular orbital (HOMO) cannot spread widely inside the C_{60} and is somewhat compressed relative to the situation in an isolated atom. As a result, the electron density at the C_{60} center is slightly higher than that of an isolated Be atom. On the other hand, when the Be atom is adsorbed under a single bond (Fig. 4, lower left), the Be2s HOMO is hybridized with the unoccupied t_{1u} orbitals of the C_{60}. When the Be atom is adsorbed under a five-membered ring (Fig. 4, middle) or a six-membered ring (Fig. 4, right), the system shows a spin polarization with a magnitude of $2\mu_B$. Their majority spin HOMO and HOMO-1 orbitals are also shown in Fig. 4. Unlike in the other cases, one of the Be2s electrons transfers to the t_{1u} orbital and expands into a large area in the C_{60} (the upper figures show the majority spin HOMO), and the other electron stays around the Be atom (the lower figures show the majority spin HOMO-1). As a result, the electron density at the Be nucleus position adsorbed under the C_{60} is less than that of an isolated Be atom. By contrast, in a Be metal, the Be2s electrons spread over the whole metal, but each Be atom contains a net portion of the Be2s electrons. Therefore, the electron density at the Be nucleus position in a Be metal is higher than in the cases where the Be atom is adsorbed under the C_{60}, away from the center of the cage.

TABLE I. The calculated electron density at the ^{7}Be nucleus position in lower and/or the lowest total energy inside the C_{60}. The electron density of an isolated Be atom and of a Be metal is also tabulated for comparison.

	Electron density	Total energy
	(e^-/Å^3)	Difference (eV)
C_{60} center	36.016	0.0 (most stable)
Under six-membered ring	35.332	0.142
Under five-membered ring	35.287	0.068
Under single bond	35.243	0.098
Be atom	35.954	-
Be metal	35.423	-

Using the total energy $E(\boldsymbol{r})$ and the electron density $\rho(\boldsymbol{r})$ calculated at each Be nucleus position $\boldsymbol{r}$ inside the C_{60}, we evaluate the electron density at Be nucleus position at temperature (T) by taking average of the densities at various Be positions according to the Boltzmann distribution. Details of the procedures for calculation will be presented elsewhere [26]. At the absolute zero temperature ($T = 0$ K), the Be atom is located at the C_{60} center and the electron density at the Be nucleus position is equal to $36.016e^-$/Å^3, while at $T = 293$ K, it is estimated as $35.899e^-$/Å^3. (The ^{7}Be atom at $T = 293$ K moves around the local minima as seen in Fig. 4 and electrons sometimes interact between Be2s and C_{60} t_{1u} states.) Then, the relative difference between them amounts to 0.33%, which can be compared with the relative difference of 0.34% for the experimentally determined half-lives (52.47 d at $T = 5$ K and 52.65 d at $T = 293$ K). On the other hand, if we com-

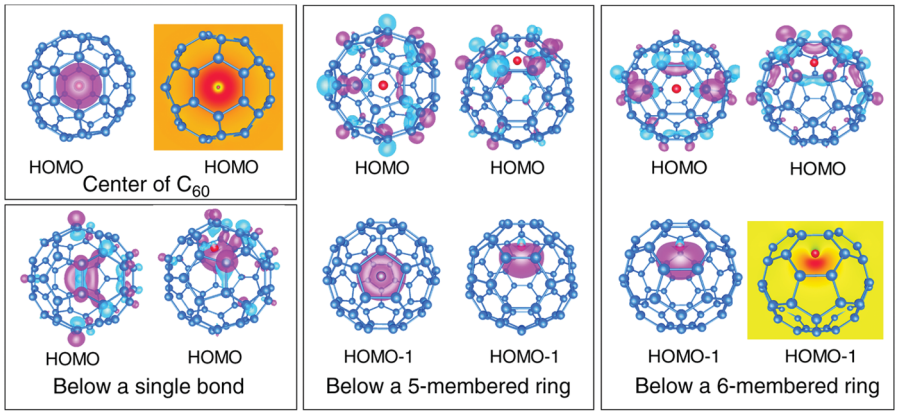

FIG. 4 (color). Schematic view of the wave functions for the HOMO (and HOMO-1) of the C_{60} molecules with a Be atom incorporated at the center (upper left, front view, and side view), below a single bond (lower left, front view, and side view), below a five-membered ring (middle, front view, and side view), and below a six-membered ring (right, front view, and side view).

pare the electron density of the ^{7}Be@C_{60} at $T = 293$ K ($35.899e^-/\text{Å}^3$) with that of Be metal ($35.423e^-/\text{Å}^3$, even also at $T = 293$ K), the relative difference between them amounts to 1.3%. This value can be also compared to the relative difference 1.1% in the experimentally determined half-lives (52.65 d for the ^{7}Be@C_{60} and 53.25 d for the Be metal (^{7}Be) on average in Fig. 3). The agreement between the theoretical and the experimental results is fairly good.

The L/K capture ratio (i.e. the ratio of electron density of L(Be2s) and K(Be1s) orbits at the Be nucleus position) is estimated to be almost 10% in the isolated Be atom [27,28]. In our theoretical calculation, we also found that the ^{7}Be atom stays at the center (potential minimum) of the C_{60} and the Be2s electrons can be fully restricted to the Be nucleus at $T = 0$ K as in an isolated Be atom ($1s^2$, $2s^2$), even though the calculated electron densities at the Be nuclear position are somewhat different [26]. On the other hand, chemically and/or metallically bonded Be atoms always lose Be2s electron to some degree, due to their alkali-earth nature (relatively smaller electronegativity). Therefore, the L/K capture ratio in the ^{7}Be atom is reduced when the ^{7}Be is chemically bonded and/or inside host metal materials [3–16]. Here, the magnitude of the average charge transfer from the L(Be2s) electrons of the ^{7}Be atom may play an important role for such variation in the decay constant in the environments.

In summary, the EC-decay rate of ^{7}Be in C_{60} at $T = 5$ K and in Be metal (^{7}Be) at $T = 293$ K was measured with a reference method. We found that the half-life of the ^{7}Be in the ^{7}Be@C_{60} cooled to $T = 5$ K, 52.47 ± 0.04 d, breaks the previous half-life record by more than 0.3%, and that the ^{7}Be decay speed in the ^{7}Be@C_{60} at $T = 5$ K is nearly 1.5% faster than that in the Be metal (^{7}Be) at $T = 293$ K. From the theoretical calculation, the most stable position of the Be atom inside the C_{60} is the center, and the electron density at the Be nucleus position is the highest even at the low temperature. In this case, we would like to emphasize that we have observed the nuclear decay rate of a ^{7}Be nucleus surrounded by a ($1s^2$, $2s^2$) electron shell which is almost that of an isolated atom.

The authors are grateful to the staff at the Accelerator Divisions of the Laboratory of Nuclear Science and the Cyclotron Radio-Isotope center, Tohoku University. This work was supported by Grants-in-Aid for Co-operative Research No. 10640535, No. 12640532, and No. 17350024 from the Ministry of Education of Japan, the REIMEI Research Resources of JAERI, and by the Mitsubishi Foundation.

[1] E. Segré, Phys. Rev. **71**, 274 (1947).
[2] E. Segré and C. E. Wiegand, Phys. Rev. **75**, 39 (1949).
[3] H. W. Johlige *et al.*, Phys. Rev. C **2**, 1616 (1970).
[4] W. K. Hensley *et al.*, Science **181**, 1164 (1973).
[5] F. Lagoutine *et al.*, Int. J. Appl. Radiat. Isot. **26**, 131 (1975).
[6] M. Jaeger *et al.*, Phys. Rev. C **54**, 423 (1996).
[7] A. Ray *et al.*, Phys. Lett. B **455**, 69 (1999).
[8] C. A. Huh, Earth Planet. Sci. Lett. **171**, 325 (1999).
[9] L. Liu *et al.*, Earth Planet. Sci. Lett. **180**, 163 (2000).
[10] E. B. Norman *et al.*, Phys. Lett. B **519**, 15 (2001).
[11] A. Ray *et al.*, Phys. Lett. B **531**, 187 (2002).
[12] Z. Y. Liu *et al.*, Chin. Phys. Lett. **20**, 829 (2003).
[13] A. Ray *et al.*, Phys. Rev. C **73**, 034323 (2006).
[14] B. N. Limata *et al.*, Eur. Phys. J. A **27**, 193 (2006).
[15] Y. Nir-El *et al.*, Phys. Rev. C **75**, 012801(R) (2007).
[16] J. A. Tossell, Earth Planet. Sci. Lett. **195**, 131 (2002).
[17] T. Ohtsuki *et al.*, Phys. Rev. Lett. **77**, 3522 (1996).
[18] T. Ohtsuki *et al.*, Phys. Rev. Lett. **93**, 112501 (2004).
[19] T. Braun and H. Rausch, Chem. Phys. Lett. **237**, 443 (1995).
[20] T. Ohtsuki *et al.*, Phys. Rev. Lett. **81**, 967 (1998).
[21] T. Ohtsuki *et al.*, J. Chem. Phys. **112**, 2834 (2000).
[22] T. Ohtsuki (to be published).
[23] B. Delley, J. Chem. Phys. **113**, 7756 (2000).
[24] A. D. Becke, J. Chem. Phys. **88**, 2547 (1988).
[25] C. T. Lee *et al.*, Phys. Rev. B **37**, 785 (1988).
[26] T. Morisato *et al.* (to be published).
[27] P. A. Voytas *et al.*, Phys. Rev. Lett. **88**, 012501 (2001).
[28] A. Ray *et al.*, Phys. Rev. C **66**, 012501(R) (2002).